NASA TN D-1803

23 p.

TECHNICAL NOTE

D-1803

INVESTIGATION OF THE EFFECTS OF VARIABLE-AMPLITUDE LOADINGS ON FATIGUE CRACK PROPAGATION PATTERNS

By C. Michael Hudson and Herbert F. Hardrath

Langley Research Center
Langley Station, Hampton, Va.

NATIONAL AERONAUTICS AND SPACE ADMINISTRATION
WASHINGTON

August 1963

NATIONAL AERONAUTICS AND SPACE ADMINISTRATION

TECHNICAL NOTE D-1803

INVESTIGATION OF THE EFFECTS OF VARIABLE-AMPLITUDE LOADINGS ON FATIGUE CRACK PROPAGATION PATTERNS

By C. Michael Hudson and Herbert F. Hardrath

SUMMARY

Axial-load variable-amplitude fatigue tests were conducted on 2024-T4 aluminum-alloy specimens. Both gust and ground-air-ground cycles were simulated in these tests, and the resulting fracture patterns were carefully inspected to determine which loadings produced the various markings. The effects of loading order and load magnitude on the size and texture of the markings were also investigated.

INTRODUCTION

The fracture surfaces of structural components which fail in fatigue frequently exhibit the "tide" markings such as those in figure 1, which is a photograph of an aircraft spar cap which failed in service. These markings were produced by the various load cycles to which the structure was subjected while in service. If some means were available for interpreting these markings in terms of the loadings required to produce them, airline operators could more definitely establish safe inspection intervals for their airplanes.

The most feasible method of interpreting these service markings was to apply predetermined load cycles to specimens containing fatigue cracks of known length and, subsequently, to determine the size and texture of the resulting markings. Towards this end, a series of axial-load variable-amplitude fatigue tests were conducted on specimens made of 2024-T4 aluminum alloy. In the first three tests, gust cycles were simulated and the effects of load magnitude and order of loading on the crack propagation pattern were investigated. In the fourth test, simulated ground-air-ground cycles were added to determine whether this kind of loading affected the resulting pattern. For the fifth test, a loading spectrum representing 1,000 flight hours was continuously repeated to determine how long a fatigue crack would propagate before causing the specimen to fail.

SPECIMENS AND TESTS

Specimens

Test specimens were made from 2024-T4 aluminum-alloy bar stock and were machined to have a cross section representative of an aircraft spar cap. The tensile properties of the material tested are as follows:

Yield stress (0.2-percent offset), ksi	46.2
Ultimate strength, ksi	64.8
Total elongation, 2-inch gage length, percent	20.9
Young's modulus, ksi	10.2×10^3
Number of specimens	34

The general configuration of the specimens may be seen in figure 2. The specimens were from the same lot used in a previous investigation of residual static strength of specimens containing fatigue cracks. (See ref. 1.) The central portion of each specimen was 2 inches wide and 3/4 inch thick with tangs 1 inch in width and either 1/8 or 1/4 inch thick extending from each edge. A 1/4 inch-diameter hole was drilled in the center of each tang. The material between the hole and the edge of the specimen was sawed away on one side of each specimen. A 0.005-inch-radius notch was then cut into the inner side of the hole in order to accelerate crack initiation. This notch was produced by repeatedly drawing a thread impregnated with valve-grinding compound across the inner side of the hole.

Equipment

The fatigue testing machine employed in this investigation is shown in figure 3. This machine is capable of applying a maximum static preload of ±66 kips through an electrically driven screw which adjusts the force in a spring. Alternating loads up to ±44 kips were applied at rates up to 4,000 cpm by using the subresonant loading system incorporated in the machine. Alternating loads up to ±66 kips were applied hydraulically at rates up to 60 cpm. The cycles counter read in hundreds of cycles for the subresonant system and in cycles for the hydraulic unit. Loads were monitored by measuring the output of a bridge circuit whose active elements were wire-resistance strain gages fixed to a dynamometer in series with the specimen. The maximum error anticipated for this monitoring system was ±1 percent.

Tests

Test specimens were subjected to repeated axial loads producing nominal stresses of 10 ± 3 ksi until cracks had initiated and propagated through one tang into the central section of the specimen. The loading schedule for each specimen was then changed to determine the effect of various types of loading on the crack propagation pattern. It should be noted here that all stresses are referred to the original net cross section of the specimens. In order to identify the markings produced by each type of loading, the crack lengths were measured at the

surface of the specimen each time the load was changed. Whenever gust loadings were being simulated, the mean stress was 10 ksi, which is the value chosen as representative of the 1g stress which might occur in an aircraft.

The loading schedules consisted primarily of low-amplitude cycles (10 ± 3 ksi) applied several thousand at a time. Individual cycles of higher amplitude were interposed at predetermined intervals to study their effects on the crack propagation pattern. In the first three tests, the single cycles were representative of gust-load cycles in that they were symmetrical about the 10-ksi mean stress. The highest load cycle applied in a given test was varied to systematically study its effect. The fourth test emphasized loadings representative of the ground-air-ground cycle, which was assumed to fluctuate between 12 ksi and -5 ksi. A fifth test was conducted by using a loading program representative of gust-load experience in a twin-engine airliner. Each test sequence is described in more detail in the section entitled "Individual Tests."

RESULTS

General

The results of this investigation are presented in figures 4 to 8. Parts (a) of figures 4 to 7 and figure 8 show the fracture surfaces of the specimens tested. In order to facilitate the inspection of these figures, each significant marking on the fracture surfaces has been indexed with a capital letter. These letters refer to the portions of the loading programs which produced the markings and are described in detail in the accompanying program descriptions. By comparing the letters on the photographs with those in the descriptions, the loading program can be correlated to the fracture pattern.

The correlation of the fracture patterns with the loading programs was greatly facilitated by taking the measurements of the external crack lengths following each loading. The crack fronts were found to be continuous across the specimens, and by knowing the position of the fronts before and after a loading was applied, the increase in crack length was easily ascertained. The program-pattern correlation was further aided by the color and texture of the resulting markings. The dark markings, which indicate areas of brittle fracture, occurred only during the application of some of the high individual load cycles. On the other hand, the bright markings resulted primarily from the application of several thousand low-amplitude cycles. The contrast between the markings served to define the effects of the different loadings on the fracture pattern.

In order to further clarify the relationship of the loading program and the crack propagation pattern, parts (b) and (c) of figures 4 to 7 were added. These parts show graphically the loading program and the resulting crack growth, respectively. In part (b) the horizontal lines represent the thousands of constant-amplitude cycles (10 ± 3 ksi) applied whereas the vertical lines represent the interposed individual load cycles. Each portion of the loading history is again labeled with a capital letter identifying it with the portion of the fatigue fracture surface which it produced. The crack lengths in part (c) were measured

along the center line of the cross section of the specimen. The edge of the thread-cut notch was used as the reference from which crack lengths were measured.

Parts (b) and (c) were omitted from figure 8 since the primary concern in the fifth test was the study of remaining fatigue life following crack initiation.

Individual Tests

Test 1.- The purpose of test 1 was to determine whether single simulated gust cycles could produce discernible amounts of crack growth. The resulting fracture pattern is shown in figure 4(a). The individual gust cycles having magnitudes of 10 ± 10 ksi or greater produced visible amounts of brittle crack growth (B, D, E, F, and G). Note the crack growth resulting from the eight 10 ± 10 ksi cycles applied in part E of this test. These eight loadings produced the eight small but quite distinct amounts of brittle crack growth seen in area E. The significance of these markings will be readily seen in the comparison of the results of tests 1 and 2. For convenience, these eight increments of brittle crack growth in area E have been represented in figure 4(c) by a continuous line rather than by one containing eight discrete steps.

In the final stages of fatigue life a considerable amount of crack growth resulted from a cycle having a magnitude of only 10 ± 7.6 ksi. Brittle crack growth at this low stress level was probably due to the large stress concentration at the tip of the crack and the high net section stress.

Test 2.- The purpose of test 2 was to determine the specific amounts of crack growth which would result from loadings of various magnitudes. The amplitudes of the single cycles of load applied were in the sequence 10, 8, 6, 4, 2, 10, 8, 6, 4, 2, . . . ksi. Figure 5(a) shows the fracture surface which resulted from this test. Again, only the gust cycles having magnitudes of 10 ± 10 ksi or greater produced visible increments of brittle crack growth (B, D, F, H, J, and L). However, the amounts of crack growth which resulted from each 10 ± 10 ksi cycle were considerably greater than those which resulted from cycles of the same magnitude in test 1. It was suspected that a difference in the residual stresses resulting from the loadings applied prior to the 10 ± 10 ksi cycles effected this differential crack propagation.

Test 3.- Test 3 was conducted to study in more detail how previous loading history affected succeeding crack propagation. With minor variations, the schedule of amplitudes of single gust cycles was 6, 8, 6, 4, 8, 6, 4, . . . ksi. The resulting fracture pattern, shown in figure 6(a), indicated that the 10 ± 6 ksi cycle applied immediately after the initial crack growth produced a small but measurable amount of brittle crack growth (B). Brittle propagation again occurred with the application of the subsequent 10 ± 8 ksi cycle (D). However, the next 10 ± 6 ksi cycle produced no visible crack extension. Another 10 ± 8 ksi cycle was applied (F), followed by a 10 ± 6 ksi cycle, and again the latter cycle failed to produce any visible crack extension. This sequence was repeated once more with two 10 ± 6 ksi cycles following the 10 ± 8 ksi cycle (H). That time the first 10 ± 6 ksi cycle caused no visible crack growth, however, the second 10 ± 6 ksi cycle (J) did.

The results of these first three tests indicate that the amount of crack growth resulting from a given load cycle depended upon both the magnitude of the loading cycle and the previous loadings to which the specimen had been subjected. Generally, only the highest stresses produced markings, at least until the crack had grown through about 1/3 of the section. A mechanism which offers an explanation of this phenomenon will be discussed in a subsequent section.

Test 4.- Test 4 was conducted to determine the effect of simulated ground-air-ground cycles on crack propagation. As indicated previously, ground-air-ground cycles were assumed to range from 12 to -5 ksi. Twenty such cycles were applied as indicated by the vertical lines extending below the zero stress line in figure 7(b). In addition, 4 cycles of 10 ± 10 ksi were applied singly early in the test. Figure 7(a) shows that the 20 ground-air-ground cycles produced no detectable crack extension until the final stages of fatigue life. Even then, 10 ± 3.5 ksi cycles produced larger markings than the ground-air-ground cycles. Apparently, the maximum stress in a cycle has a much greater influence on the texture of the fracture than does the amplitude.

Test 5.- The purpose of test 5 was to estimate the number of simulated flight hours over which a fatigue crack might propagate before causing failure. This estimate was made by using a test program which simulated 1,000 hours of flight history of a twin-engine airliner. The loading program was formulated by using a gust frequency spectrum (ref. 2) to determine the number of cycles to be applied at each of five preselected load levels to simulate the loading history for 1,000 flight hours. Once the number of cycles for each load level had been determined, each number was divided into 30 equal units. A table of random numbers was then used to determine the sequence in which each unit was applied. The amplitudes of the cycles and the total number of cycles in 1,000 hours for each load level are shown in the following table:

Alternating stress, ksi	Number of cycles to simulate 1,000-hour load history
10.6	3
7.5	25
5.3	252
3.7	2,520
2.0	25,200

As in the previous tests, a mean stress of 10 ksi was used to simulate the 1 g stress. For succeeding 1,000-hour increments, the loading program was simply repeated.

Figure 8 shows the fracture surface which resulted. The fatigue crack was initiated and propagated through the tang to the point A (fig. 8) at the constant stress level of 10 ± 3 ksi. The programed loading was then begun and continued until the specimen failed after the accumulation of load cycles statistically approximating the load experience for 18,700 flight hours. Examination of the fracture surfaces indicates that the bright area of ductile fracture (B) was

produced by all the load cycles representing the first 15,000 hours of flight history. Only very faint markings are discernible in this area. They are believed to result from discrete applications of the highest gust cycles in the program, the magnitude of which was 10 ± 10.6 ksi. These 10 ± 10.6 ksi cycles produced very distinct markings on the fracture surface in subsequent repetition of the loading program. Cycles of this magnitude occurred three times in each repetition of the loading schedule. Counting backward from the third application of this loading during the 19th repetition when the specimen failed indicates that the dark bands U and W resulted from the first two applications of the 10 ± 10.6 ksi cycles in the 19th repetition. Similarly, bands O, Q, and S occurred in the 18th repetition; bands I, K, and M in the 17th; and bands C, E, and G in the 16th. Measurements of the exterior crack lengths made during testing substantiated this correlation of the loading program and the fracture pattern. The bright areas seen alternating with the dark brittle bands were produced by the part of the loading program between the high stress cycles.

DISCUSSION

Inspection of the crack propagation patterns found on the fracture surfaces of all five specimens gave an insight into the way fatigue cracks propagate. The high individual stress cycles produced brittle crack growth principally in the center of the specimens. The most obvious explanation of this variation in crack growth was a variation in the stress field along the crack front. The cause of this variable stress field is as follows. The application of a tensile loading to the specimens produced a tensile stress which was magnified along the fracture front by the crack-induced stress concentration. As the tensile stress increased, the amplified stress along the fracture front exceeded the yield point and plastic deformation occurred. Figures 9 and 10, respectively, show the generalized stress-strain relationships which developed at the free sides and in the interiors of the specimens. Near the free sides deformation proceeded without hinderance, and a normal plastic stress-strain relationship, OAB, developed. However, in the interior of the specimen the plastic flow was partially restrained by the surrounding elastic material. Since the stress in the interior region could not be readily relieved by plastic deformation, it increased "hyperplastically," OAB', as the normal stress increased until the local ultimate tensile strength was exceeded. At that point the center of the crack front advanced rapidly and produced a brittle type of fracture. This rapid crack growth continued until the crack front advanced into a region of less work-hardened material. From the stress-strain relationships described, it is clear that some plastic deformation occurred in the material ahead of the advancing crack front. The significance of this yielding will be discussed in subsequent paragraphs.

The crack front was invariably advanced further into the interior of the specimen than along the edges. Consequently, the fractured area was always larger than was indicated by the exterior crack length. Thus, aircraft must be inspected very carefully in order that cracks may be detected before catastrophic failure occurs.

It was also observed that crack growth proceeded more rapidly along the sides of the specimens than in the interior during the application of the lower stress cycles. In reference 3 this same phenomenon was observed and was attributed to the high stress concentration at the trailing edge of the crack, or to the high ratio of shear stress to normal stress near the surface of the sheet as compared with that in the interior.

The results of the first three tests indicated that fatigue crack propagation at the lower stress levels was retarded by the prior application of higher stress cycles. This phenomenon probably resulted from the presence of residual compressive stresses in the material ahead of the crack. The manner in which these residual compressive stresses were generated is demonstrated in figure 11. This figure shows a generalized stress-strain diagram for the material which forms the border of the crack front following the application of the loading OABCD. As the load is applied, the material deforms elastically from point O to point A, and then plastically from point A to point B. The load is then removed and the material recovers elastically. However, since the material has been strained plastically, it cannot return to point O but rather will reach equilibrium somewhere between zero stress and zero strain. Thus, a residual compressive stress is introduced into this material. When the next load cycle is applied, the stress will increase from point D; thus, the maximum value of the tensile stress will decrease by an amount DC. For a high stress cycle the residual stress would be large, and the effect of a subsequent lower load cycle would be significantly reduced by the remaining compressive stress. A surprising feature observed in these tests is that this effect apparently persisted even after some crack growth had occurred due to the many cycles at 10 ± 3 ksi.

Thus, it has been reasonably established that previous loading history does affect subsequent crack propagation. This conclusion means that it is not possible to determine directly the magnitudes of the loadings which produce the markings found in service failures.

It should be added that although some moderately high stress cycles produced no visible markings, this does not imply that these cycles caused no crack growth. In this investigation fracture surfaces were examined under low magnification. However, in references 3 and 4, similar markings were observed with an electron microscope, and individual increments of crack growth were attributed to individual load cycles. It therefore seems possible that submicroscopic markings were produced on the fracture surfaces by these high stress cycles even though they were not visible at low magnification.

CONCLUSIONS

Examination of the fracture surfaces resulting from variable-amplitude fatigue tests on 2024-T4 aluminum-alloy specimens support the following general conclusions:

1. The prior application of high stress cycles retarded the amount of crack growth produced by subsequent lower stress cycles. Residual compressive stresses,

resulting from the high stress cycles, were the probable cause of this retardation.

2. Large amounts of brittle crack growth occurred in the interiors of the specimens during the application of some of the higher stress cycles. This brittle crack growth resulted from the elastic restraint exerted by the material surrounding the plastically deformed region. This elastic restraint, which was a maximum in the interior of the specimen, inhibited plastic flow and as a consequence the stress increased more rapidly in the interior of the specimen than at the sides. During the application of the higher stress cycles the stress in the interior region exceeded the local ultimate tensile strength and the crack front advanced by brittle fracture. This advance was halted when the crack front propagated into a region of less work-hardened material.

3. Since previous loading history was found to affect subsequent crack propagation, it does not appear possible to determine directly the magnitudes of the loadings which produce markings in service failures. On this basis it appears that analysis of such fracture markings is not a reliable technique in failure studies.

4. The ground-air-ground cycles applied in the fourth test produced no visible markings on the fracture surfaces until the final stages of crack propagation.

Langley Research Center,
National Aeronautics and Space Administration,
Langley Station, Hampton, Va., May 14, 1963.

REFERENCES

1. McEvily, Arthur J., Jr., Illg, Walter, and Hardrath, Herbert F.: Static Strength of Aluminum-Alloy Specimens Containing Fatigue Cracks. NACA TN 3816, 1956.

2. Walker, Walter G., and Copp, Martin R.: Summary of VGH and V-G Data Obtained from Piston-Engine Transport Airplanes From 1947 to 1958. NASA TN D-29, 1959.

3. Forsyth, P. J. E., and Ryder, D. A.: Some Results of the Examination of Aluminum Alloy Specimen Fracture Surfaces. Metallurgia, vol. 63, no. 377, Mar. 1961, pp. 117-124.

4. Schijve, J.: Fatigue Crack Propagation in Light Alloy Sheet Material and Structures. Rep. MP.195, Nationaal Luchtvaartlaboratorium (Amsterdam), Aug. 1960.

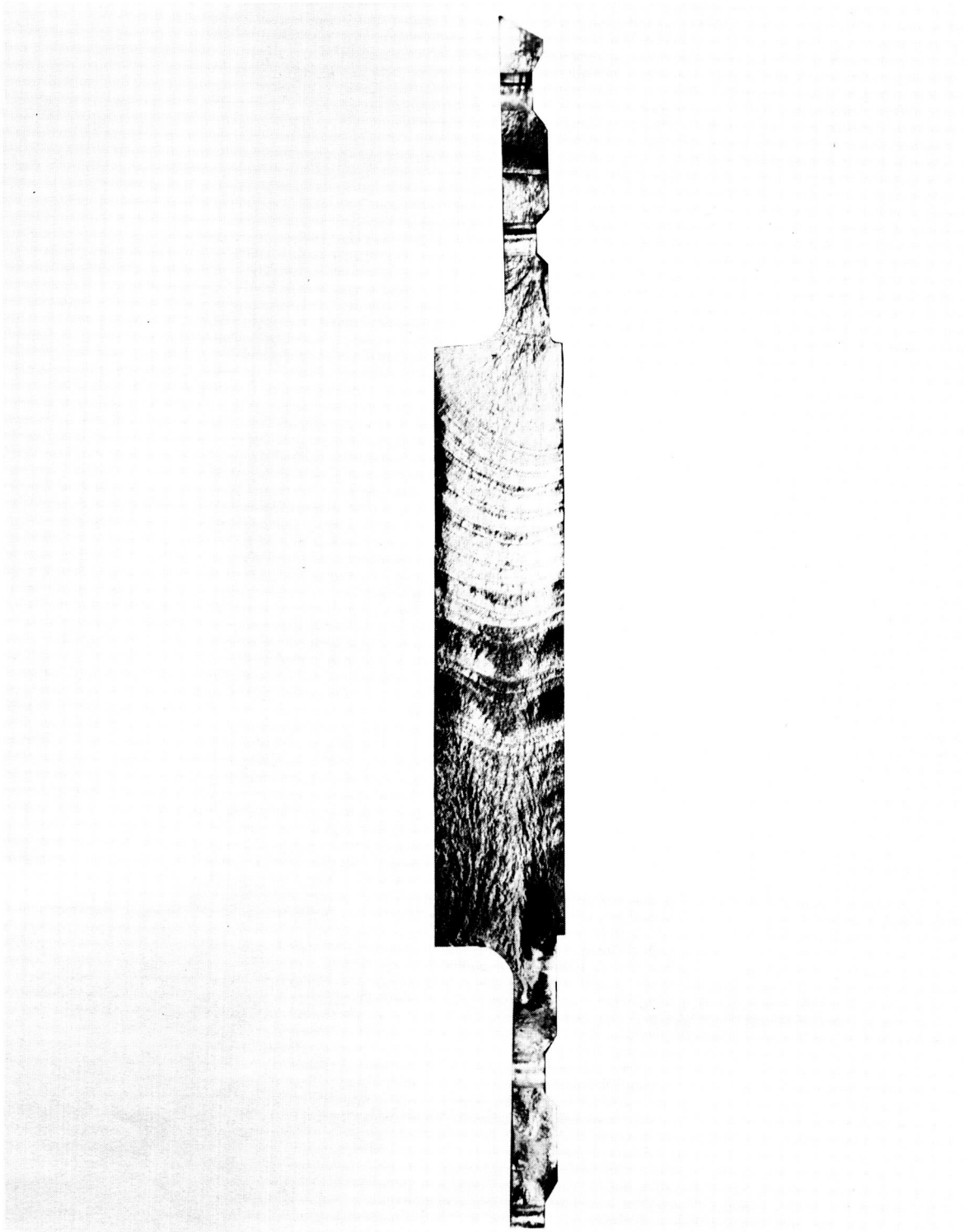

Figure 1.- Spar cap failed in service. L-63-1006

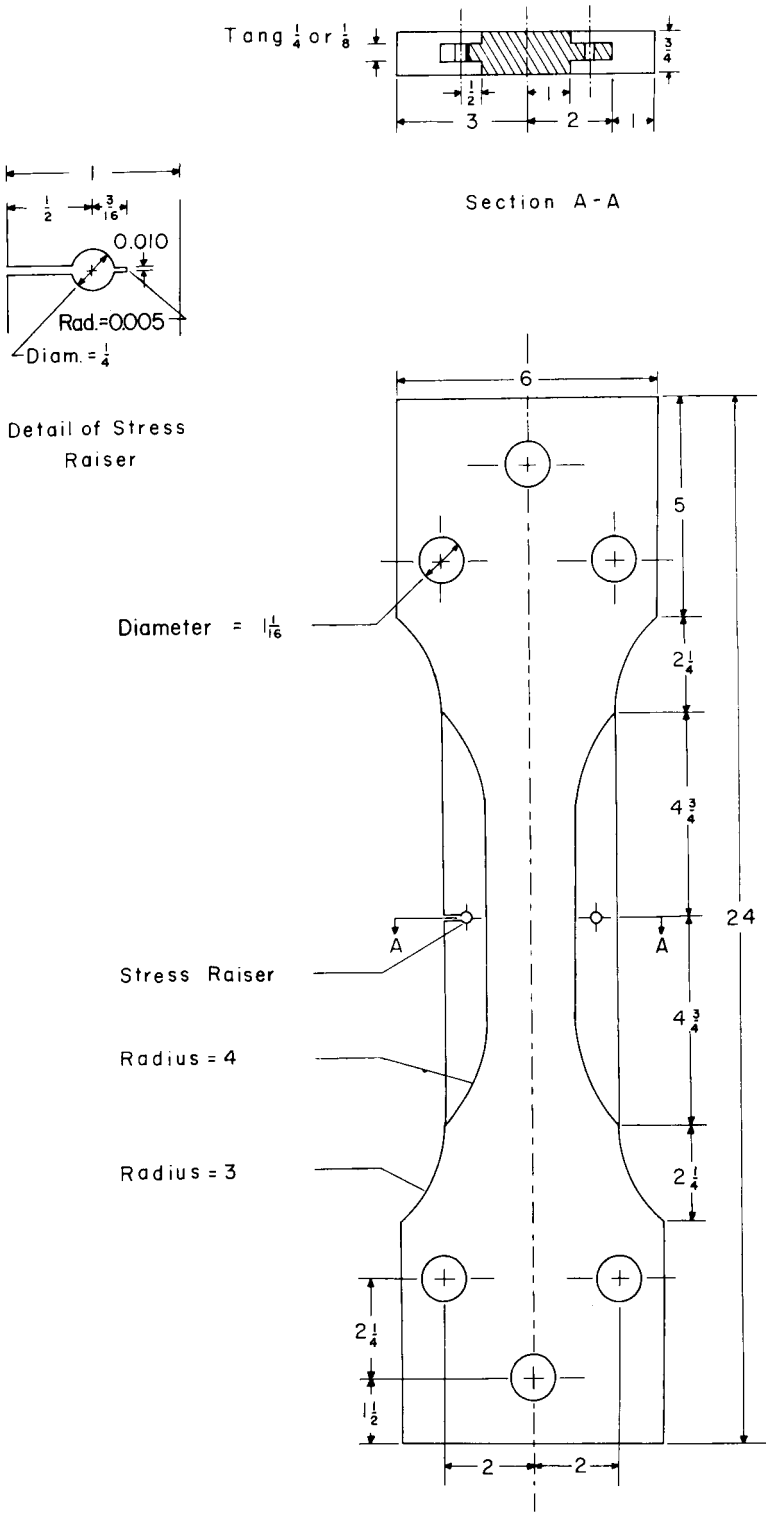

Figure 2.- Specimen configuration. All dimensions are in inches.

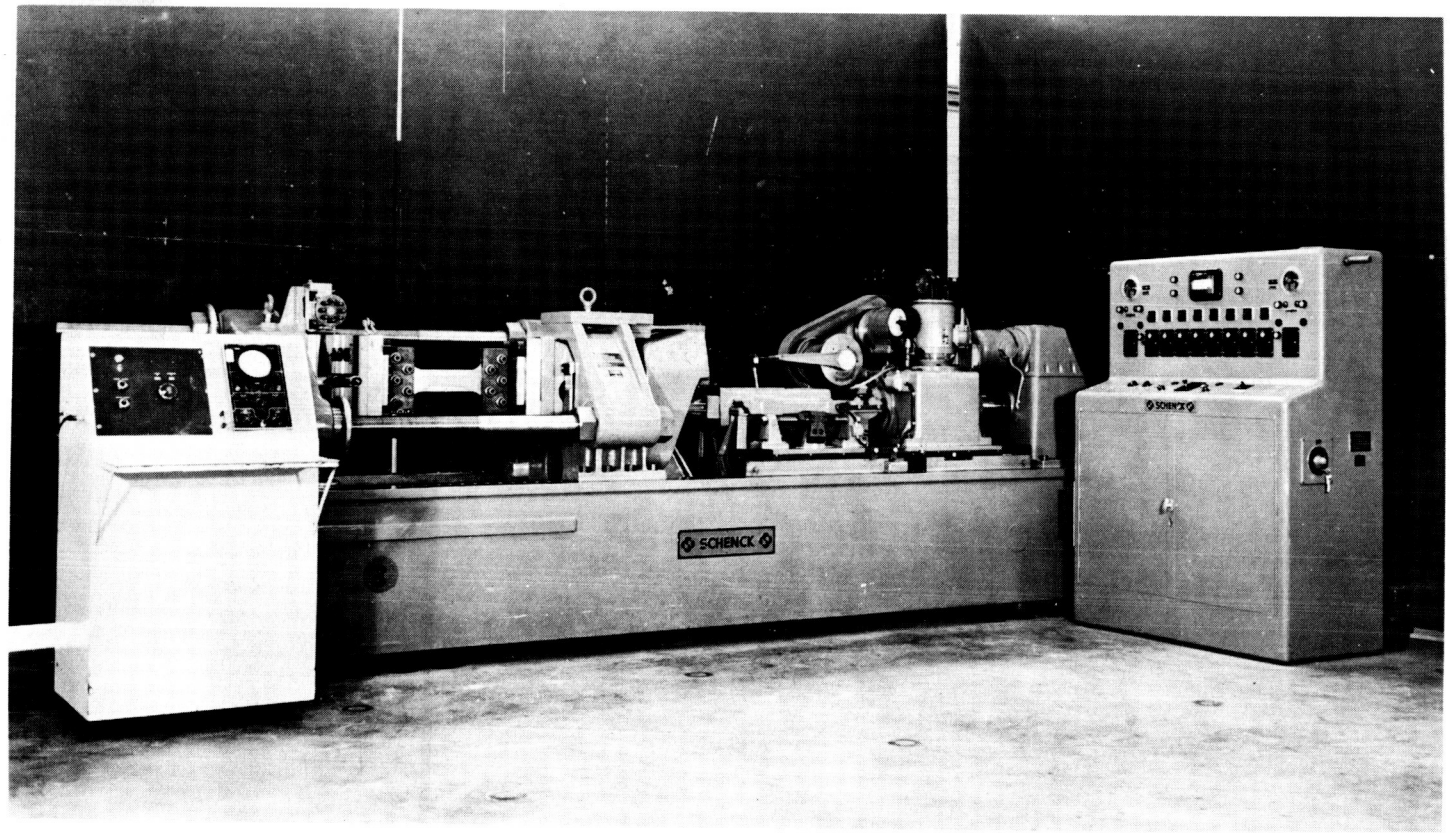

Figure 3.- Fatigue testing machine with specimen installed. L-60-2130

Test No. 1

A- 147,000 cycles at 10 ± 3 ksi
B- 1 cycle at 10 ± 13 ksi
C- 15,000 cycles at 10 ± 3 ksi
D- 1 cycle at 10 ± 13 ksi
2,000 cycles at 10 ± 3 ksi
This sequence was repeated three times.
E- 1 cycle at 10 ± 10 ksi
1,000 cycles at 10 ± 3 ksi
This sequence was repeated eight times.
F- 1 cycle at 10 ± 10.8 ksi
G- 1,000 cycles at 10 ± 3 ksi
1 cycle at 10 ± 10 ksi
This sequence was repeated twice.
1,000 cycles at 10 ± 3 ksi
1 cycle at 10 ± 5 ksi
This sequence was repeated three times.
1,000 cycles at 10 ± 2 ksi
1 cycle at 10 ± 5 ksi
This sequence was repeated twice.
1,000 cycles at 10 ± 2 ksi
H- 1 cycle at 10 ± 7.6 ksi
I- 3,000 cycles at 10 ± 2 ksi

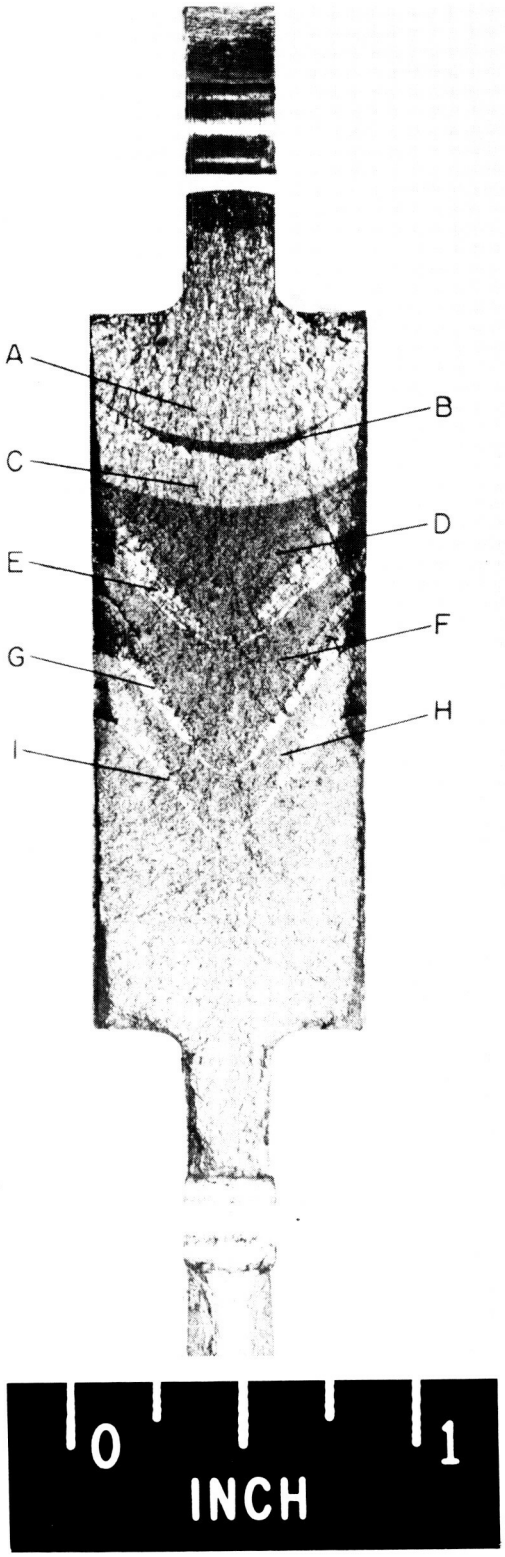

(a) Fracture surface and loading program. L-63-1001

Figure 4.- Correlation of loading program and fracture pattern for test 1.

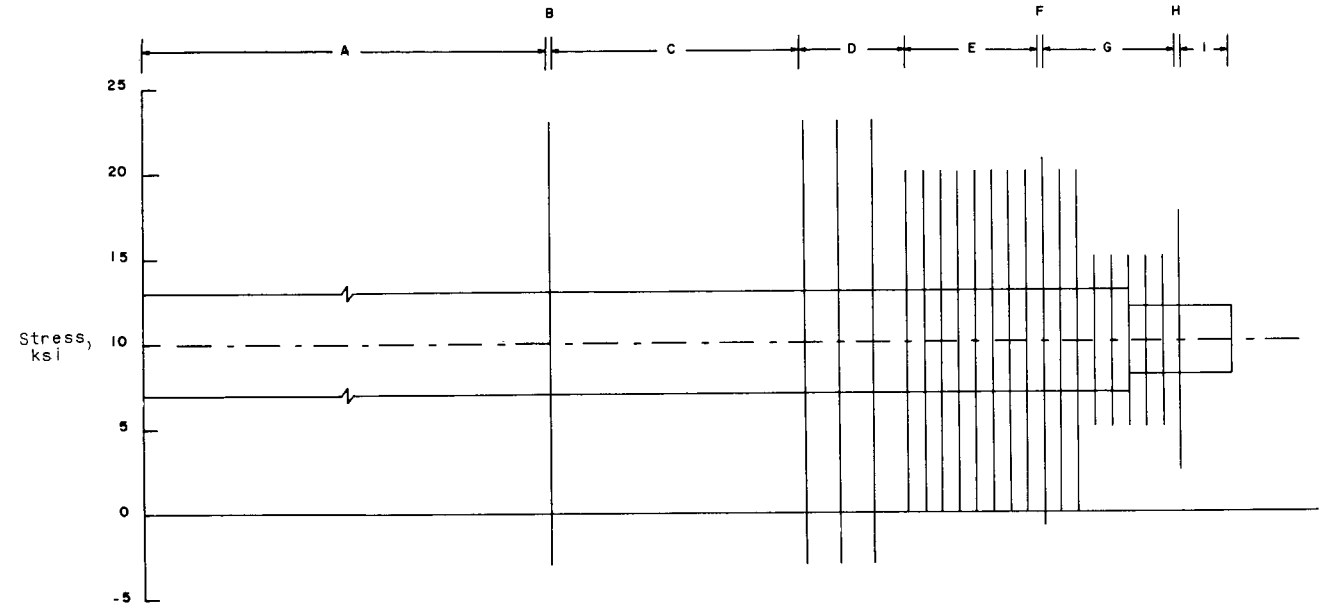

(b) Schematic of the applied loading history.

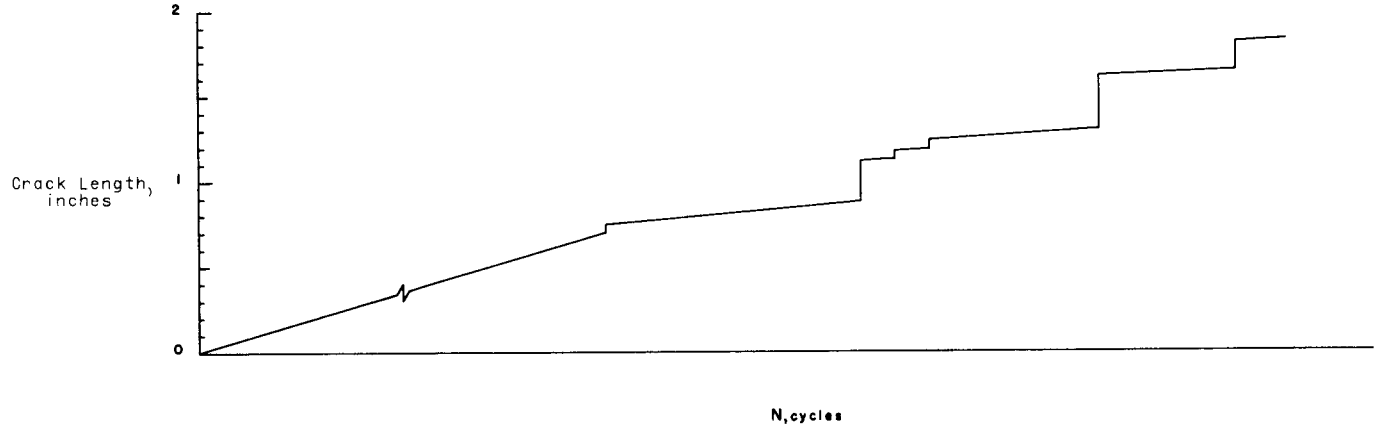

(c) Resulting crack growth.

Figure 4.- Concluded.

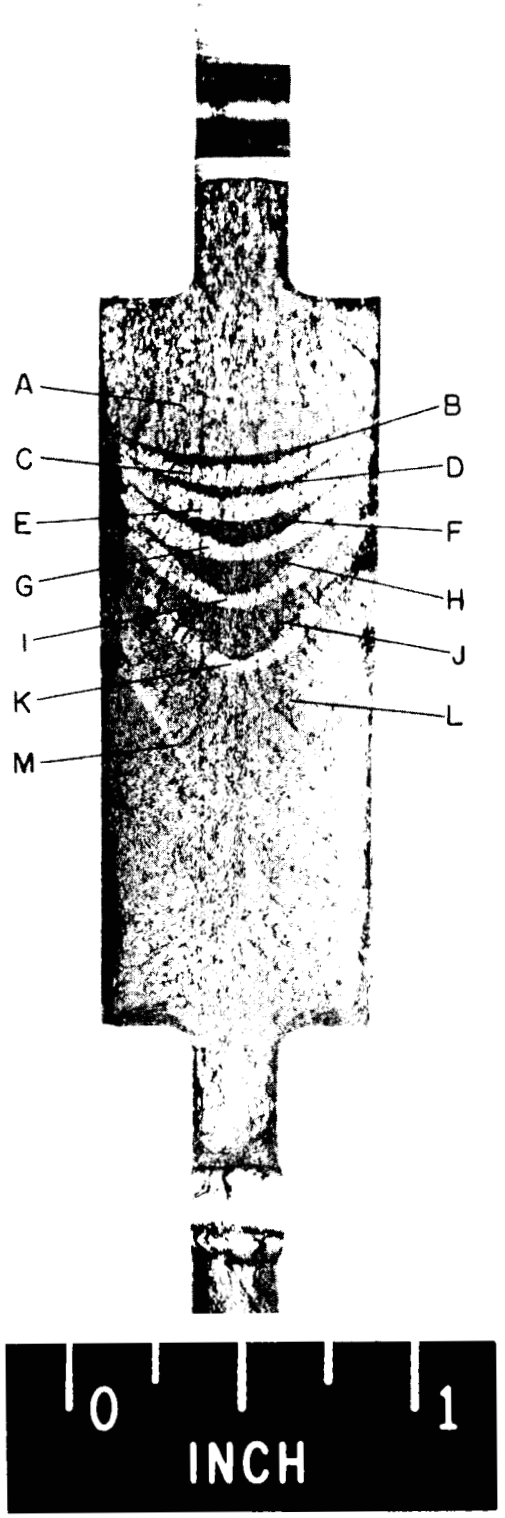

L-63-1002

(a) Fracture surface and loading program.

Test No. 2

A- 133,000 cycles at 10 ± 3 ksi
B- 1 cycle at 10 ± 10 ksi
C- 1,100 cycles at 10 ± 3 ksi
1 cycle at 10 ± 8 ksi
1,100 cycles at 10 ± 3 ksi
1 cycle at 10 ± 6 ksi
1,100 cycles at 10 ± 3 ksi
1 cycle at 10 ± 4 ksi
1,100 cycles at 10 ± 3 ksi
1 cycle at 10 ± 2 ksi
1,100 cycles at 10 ± 3 ksi
D- Same as B.
E- Same as C.
F- Same as B.
G- Same as C.
H- Same as B.
I- Same as C.
J- Same as B.
K- Same as C.
L- 1 cycle at 10 ± 11.5 ksi
M- 2,000 cycles at 10 ± 2 ksi
1 cycle at 10 ± 6 ksi
2,000 cycles at 10 ± 2 ksi
1 cycle at 10 ± 4 ksi
2,000 cycles at 10 ± 2 ksi
1 cycle at 10 ± 2 ksi
2,000 cycles at 10 ± 2 ksi
1 cycle at 10 ± 6 ksi
2,000 cycles at 10 ± 2 ksi
1 cycle at 10 ± 4 ksi
2,000 cycles at 10 ± 2 ksi
1 cycle at 10 ± 2 ksi

Figure 5.- Correlation of loading program and fracture pattern for test 2.

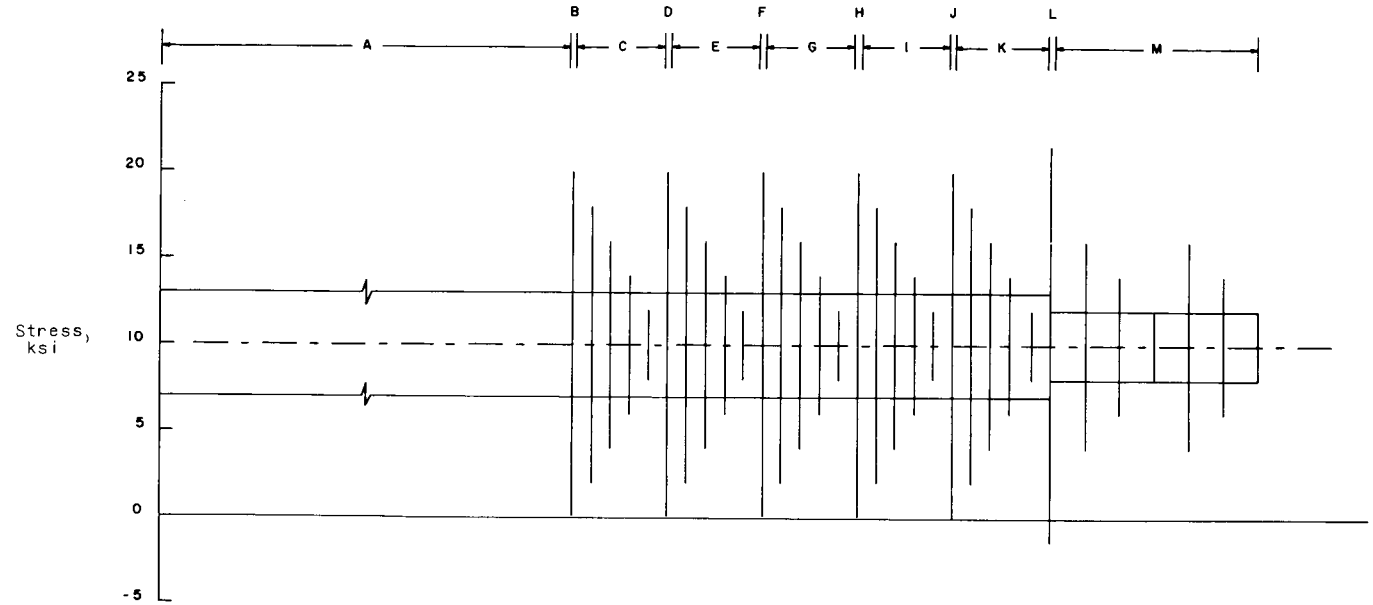

(b) Schematic of the applied loading history

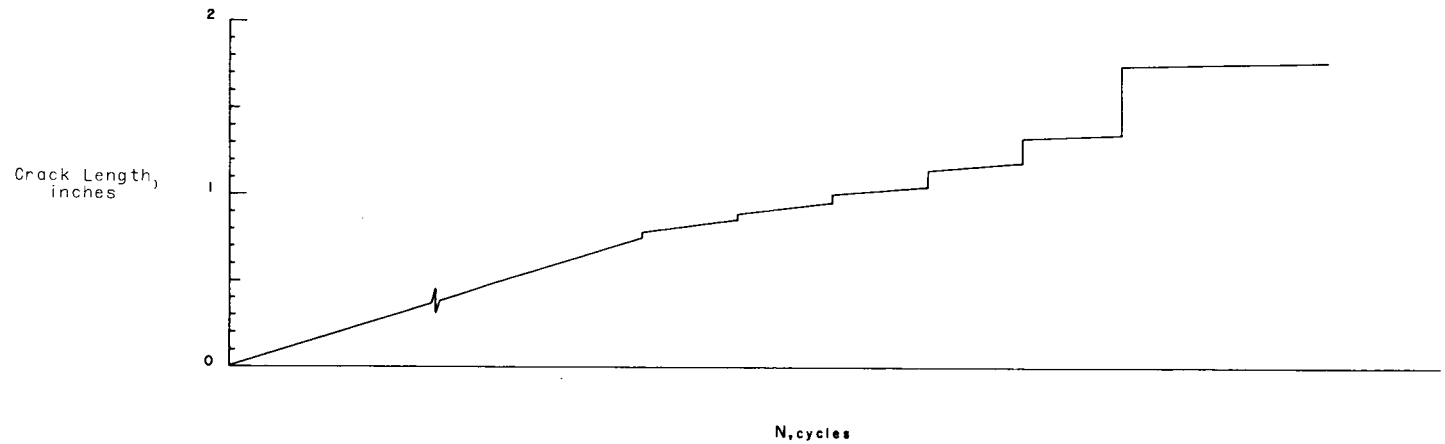

(c) Resulting crack growth.

Figure 5.- Concluded.

Test No. 3

A- 149,000 cycles at 10 ± 3 ksi
B- 1 cycle at 10 ± 6 ksi
C- 2,100 cycles at 10 ± 3 ksi
D- 1 cycle at 10 ± 8 ksi
E- 2,100 cycles at 10 ± 3 ksi
1 cycle at 10 ± 6 ksi
2,100 cycles at 10 ± 3 ksi
1 cycle at 10 ± 4 ksi
2,100 cycles at 10 ± 3 ksi
F- Same as D.
G- Same as E.
H- Same as D.
I- 2,100 cycles at 10 ± 3 ksi
1 cycle at 10 ± 6 ksi
2,100 cycles at 10 ± 3 ksi
1 cycle at 10 ± 4 ksi
2,100 cycles at 10 ± 3 ksi
J- 1 cycle at 10 ± 6 ksi
K- 2,100 cycles at 10 ± 3 ksi
L- Same as D.
M- Same as E.
N- Same as D.
O- Same as E.
P- 1 cycle at 10 ± 8.1 ksi
Q- 2,000 cycles at 10 ± 2 ksi
1 cycle at 10 ± 6 ksi
2,000 cycles at 10 ± 2 ksi
1 cycle at 10 ± 4 ksi
2,000 cycles at 10 ± 2 ksi
1 cycle at 10 ± 6 ksi
2,000 cycles at 10 ± 2 ksi
R- 1 cycle at 10 ± 6.2 ksi
S- 2,000 cycles at 10 ± 2 ksi
T- 1 cycle at 10 ± 4.7 ksi
U- 1,800 cycles at 10 ± 2 ksi

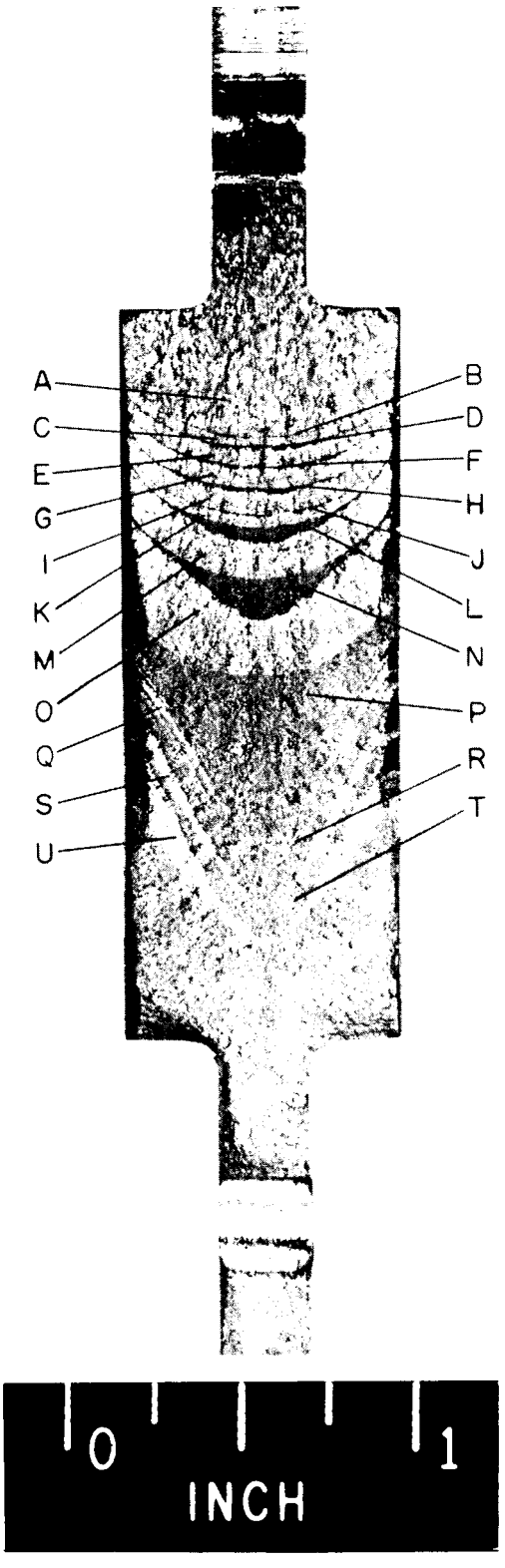

(a) Fracture surface and loading program. L-63-1003

Figure 6.- Correlation of loading program and fracture pattern for test 3.

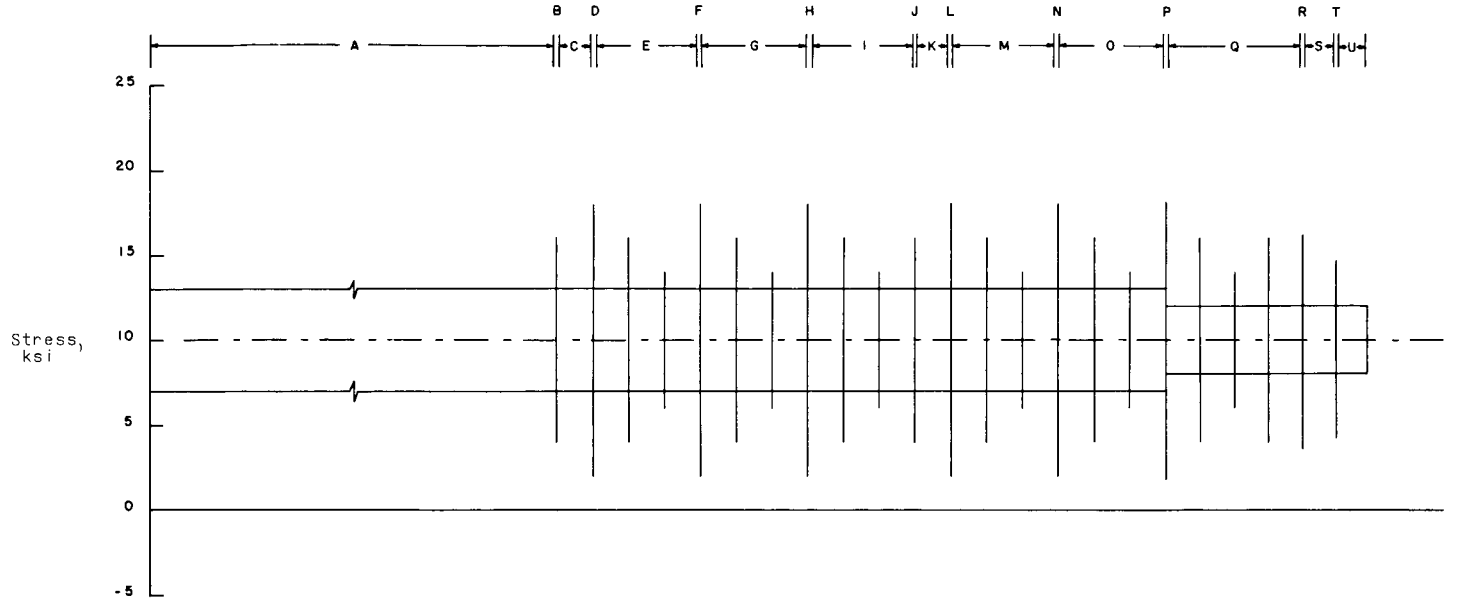

(b) Schematic of the applied loading history.

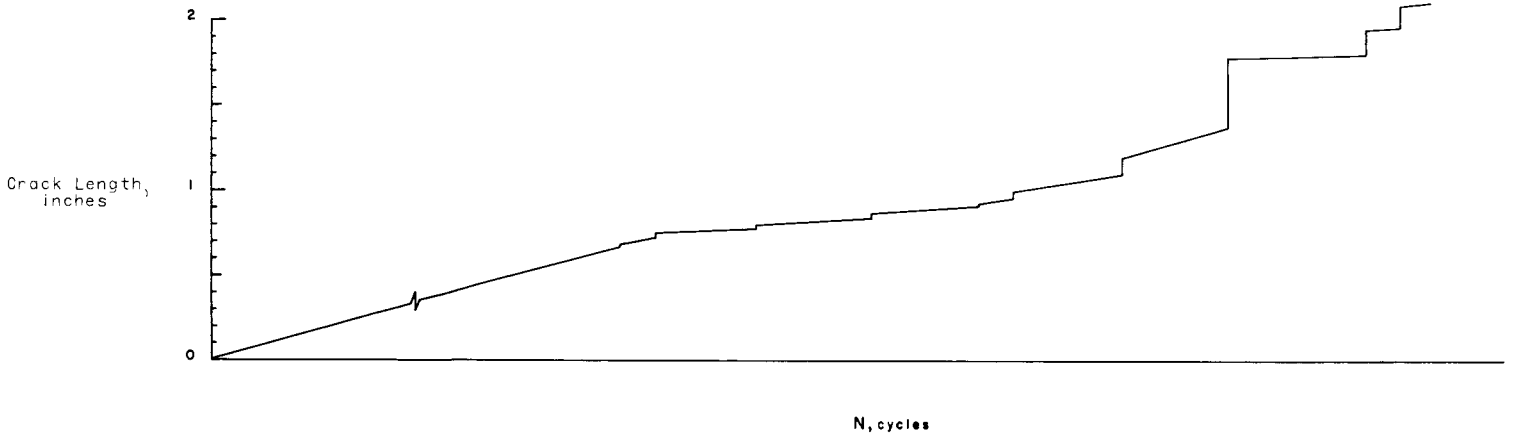

(c) Resulting crack growth.

Figure 6.- Concluded.

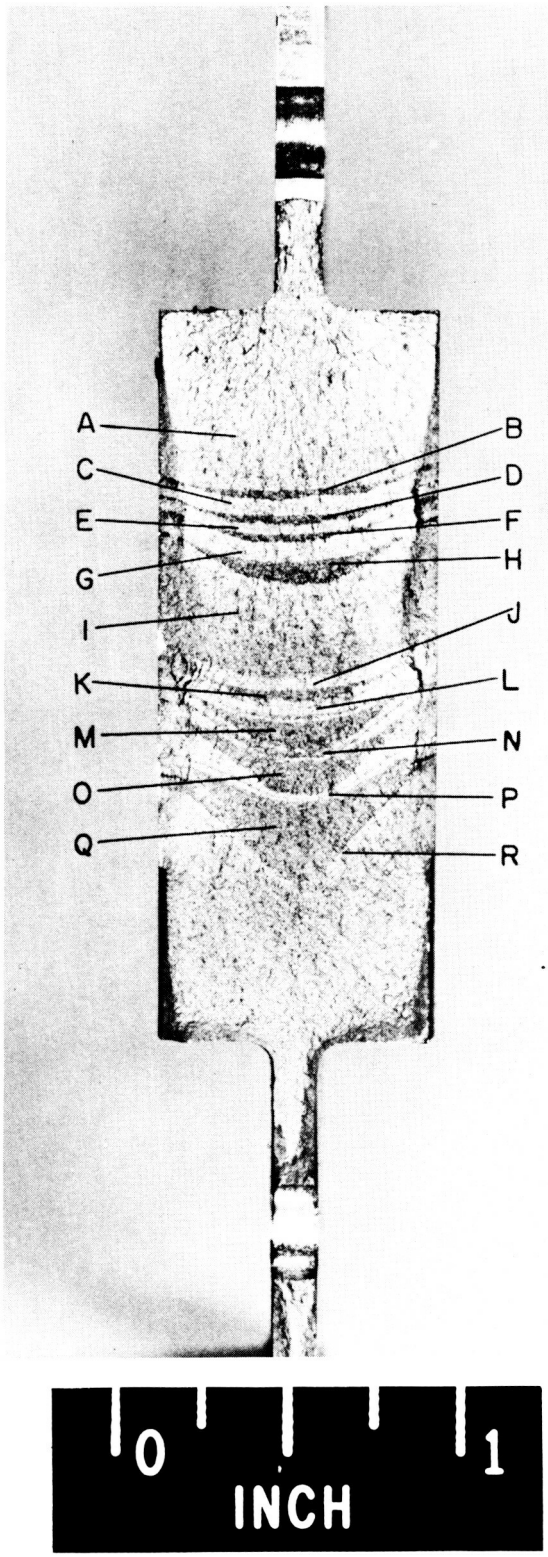

L-63-1004

(a) Fracture surface and loading program.

Test No. 4

A-	170,000 cycles	at 10	± 3	ksi
B-	1 cycle	at 10	± 10	ksi
C-	2,000 cycles	at 10	± 3	ksi
	1 cycle	at 3.5	± 8.5	ksi
	2,000 cycles	at 10	± 3	ksi
D-	Same as B.			
E-	Same as C.			
F-	Same as B.			
G-	Same as C.			
H-	Same as B.			
I-	2,000 cycles	at 10	± 3	ksi
	1 cycle	at 3.5	± 8.5	ksi
	This sequence was repeated four times.			
	4,000 cycles	at 10	± 1	ksi
	1 cycle	at 3.5	± 8.5	ksi
	This sequence was repeated five times.			
J-	4,000 cycles	at 10	± 1	ksi
	1 cycle	at 10	± 2.5	ksi
	4,000 cycles	at 10	± 1	ksi
	1 cycle	at 3.5	± 8.5	ksi
	This sequence was repeated five times.			
	4,000 cycles	at 10	± 1	ksi
K-	1 cycle	at 10	± 3.5	ksi
L-	4,000 cycles	at 10	± 1	ksi
	1 cycle	at 3.5	± 8.5	ksi
	4,000 cycles	at 10	± 1	ksi
M-	1 cycle	at 10	± 3.9	ksi
N-	Same as L.			
O-	1 cycle	at 10	± 3.4	ksi
P-	Same as L.			
Q-	1 cycle	at 10	± 3.3	ksi
R-	1,200 cycles	at 10	± 1	ksi

Figure 7.- Correlation of loading program and fracture pattern for test 4.

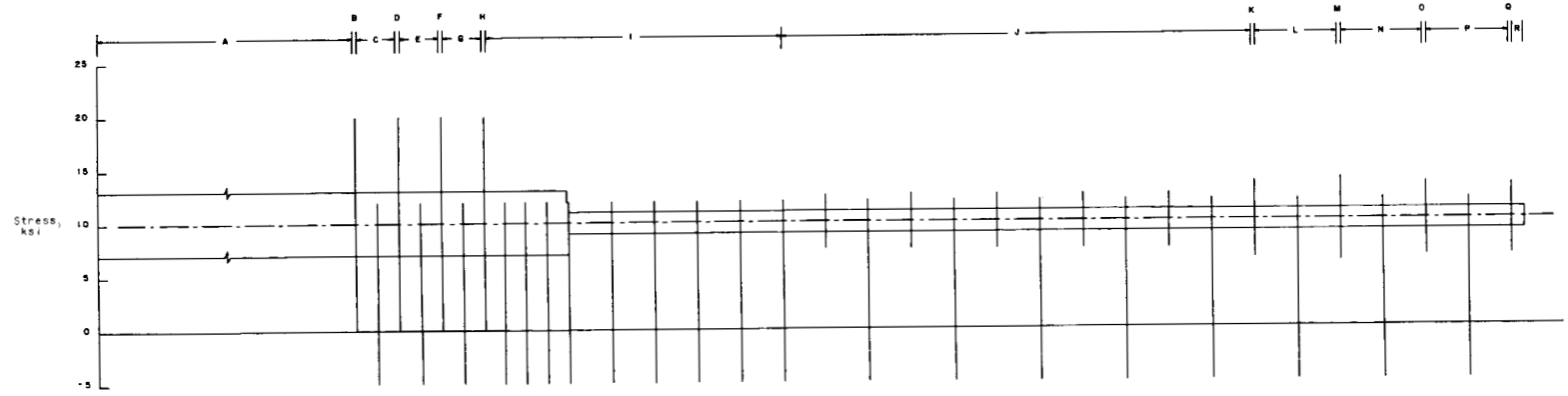

(b) Schematic of the applied loading history.

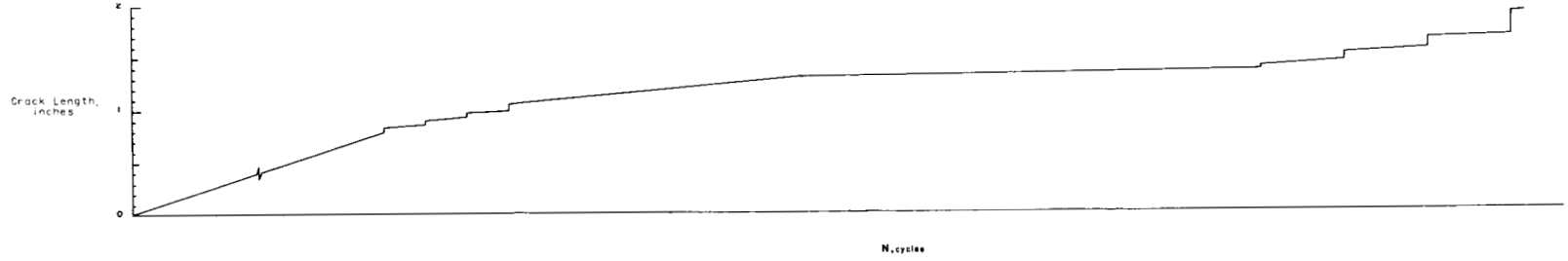

(c) Resulting crack growth.

Figure 7.- Concluded.

Test No. 5

A- Initiation of variable amplitude loadings.
B- Damage resulting from the first 15,000 simulated flight hours.
C- 1 cycle at 10 ± 10.6 ksi
D- Damage produced by the part of the loading program between each of the high stress cycles.
E- Same as C.
F- Same as D.
G- Same as C.
H- Same as D.
I- Same as C.
J- Same as D.
K- Same as C.
L- Same as D.
M- Same as C.
N- Same as D.
O- Same as C.
P- Same as D.
Q- Same as C.
R- Same as D.
S- Same as C.
T- Same as D.
U- Same as C.
V- Same as D.
W- Same as C.
X- Same as D.

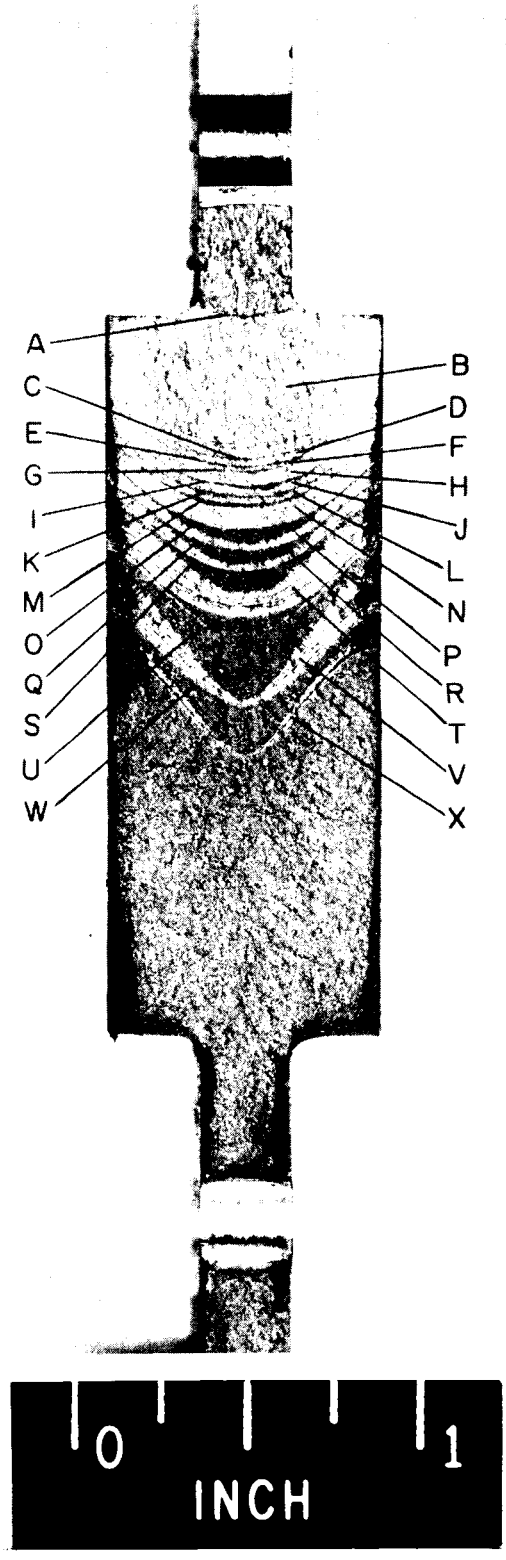

L-63-1005

Figure 8.- Correlation of loading program and fracture pattern for test 5.

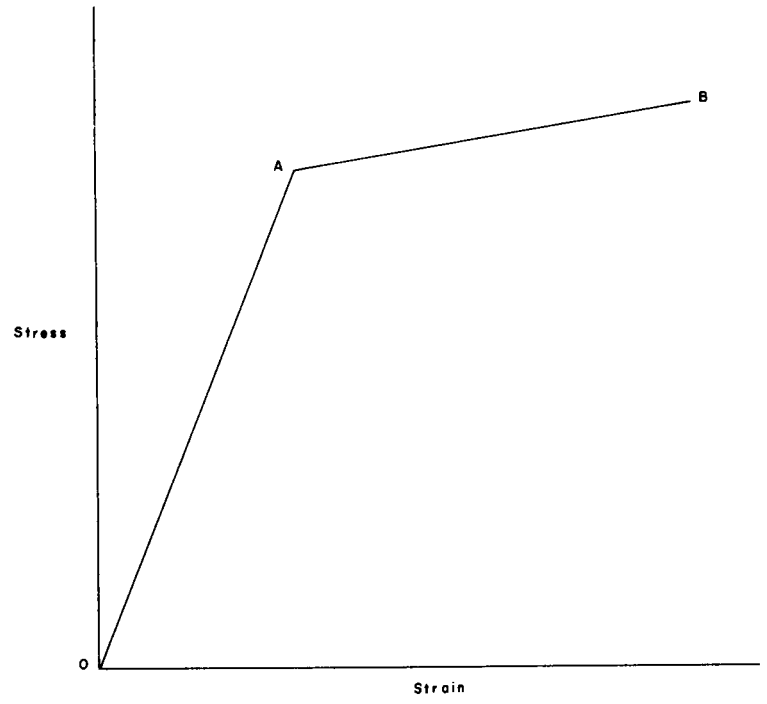

Figure 9.- Normal stress-strain relationship occurring at free sides of specimens.

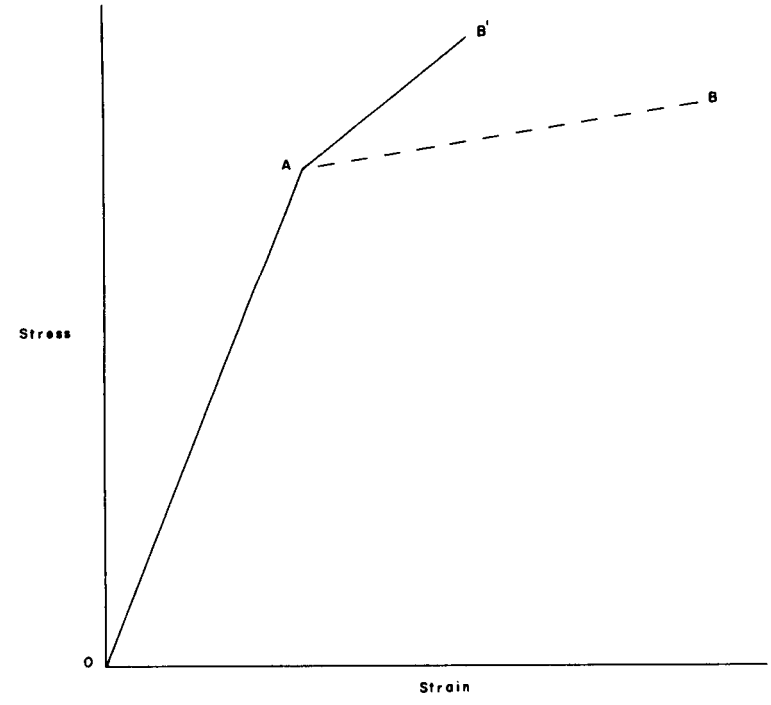

Figure 10.- "Hyperplastic" stress-strain relationship occurring in interior of specimens.

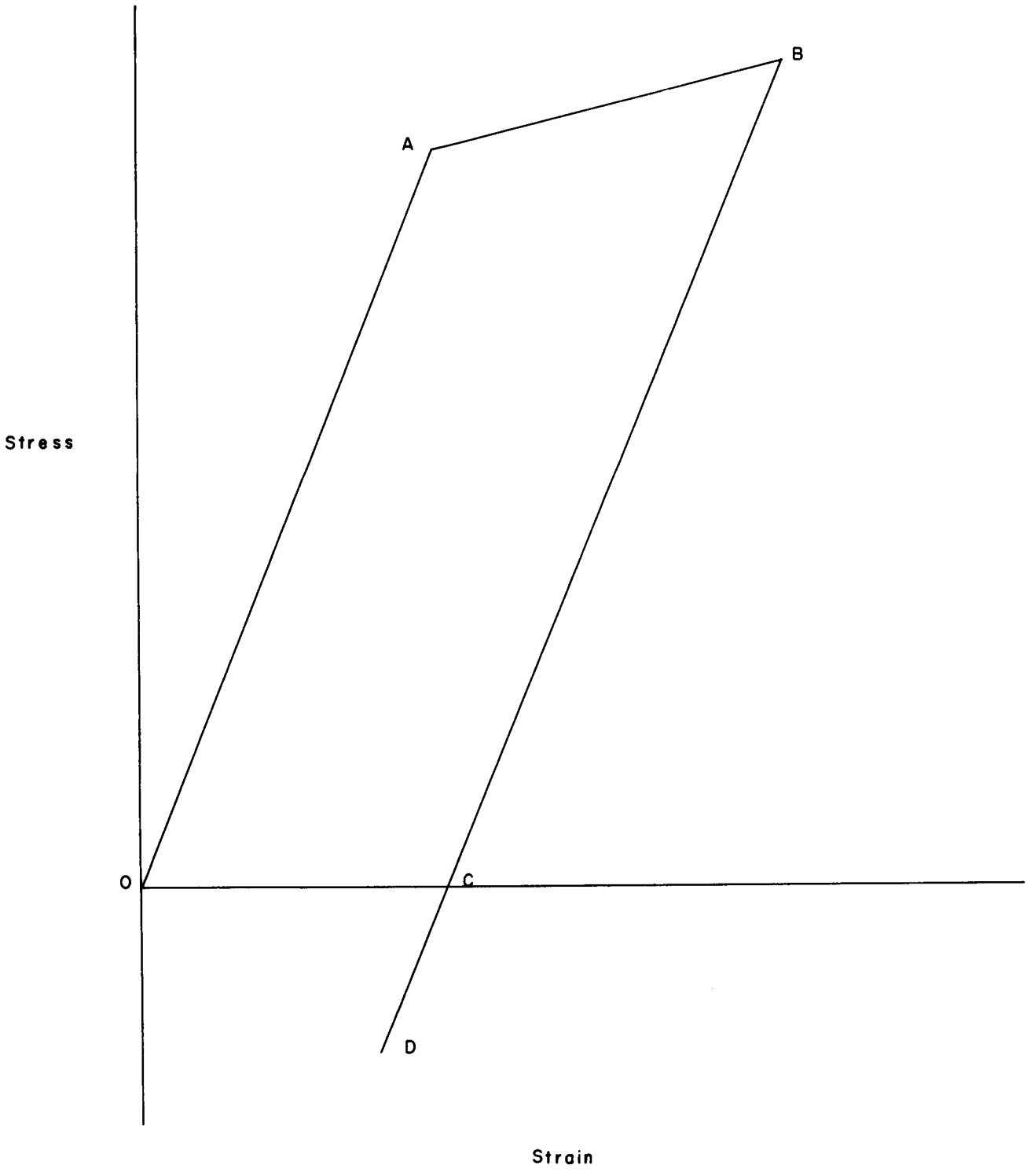

Figure 11.- Generalized stress-strain curve showing generation of residual compressive stresses.

NASA-Langley, 1963 L-1268